Available online at www.sciencedirect.com
ScienceDirect
Journal of Catalysis 252 (2007) 119–126
JOURNAL OF CATALYSIS
www.elsevier.com/locate/jcat

Research Note

Gold nanoparticles on electroless-deposition-derived MnO_x/C: Synthesis, characterization, and catalytic CO oxidation

Zhen Ma, Chengdu Liang, Steven H. Overbury, Sheng Dai *

Chemical Sciences Division, and Center for Nanophase Materials Sciences, Oak Ridge National Laboratory, Oak Ridge, TN 37831, USA

Received 13 July 2007; revised 27 August 2007; accepted 28 August 2007

Abstract

Carbon materials were modified with MnO_x via a novel self-limiting electroless deposition using $KMnO_4$ as the precursor. Gold nanoparticles were loaded onto MnO_x/C via deposition–precipitation. The resulting Au/MnO_x/C showed higher catalytic activity in CO oxidation than Au/C, and the conversion was stable on stream. The performance of Au/MnO_x/C was compared with that of Au/C, MnO_x/C, MnO_x/Au/C, Au/MnO_x, and Au/MnO_x/TiO_2, and relevant characterization, applying XRD, BET, ICP-OES, SEM, TEM, and EDX, was conducted.
Published by Elsevier Inc.

Keywords: Gold catalysis; Nanoparticles; CO oxidation; Manganese oxide; Carbon; Electroless deposition; Promoter

1. Introduction

Gold catalysts are useful for ablating pollutants, cleaning H_2 streams, and synthesizing chemicals [1–4]. The supports of choice are metal oxides, such as TiO_2, CeO_2, and Fe_2O_3 [5]. Although carbon materials are useful as adsorbents, electrodes, and catalyst supports owing to their high surface area, stability in acid and basic media, and the ease of recovering precious metals [6], carbon-based gold catalysts are seldom reported. Recently, the use of Au/C in liquid-phase oxidation of organics has been explored [7–15]. This major advance may trigger a new wave of research into Au/C-based catalysts. The activity of Au/C in CO oxidation is very low, however [14–19].

Attempts have been made to modify carbon supports before loading gold. In a 3M patent, the inventors impregnated carbon with K_2CO_3 and loaded gold through physical vapor deposition [18]. They observed enhanced activity in CO oxidation, but the origin of this promotion was not clear, and the leaching of K_2CO_3 in aqueous reactions was a problem. Kiwi-Minsker et al. [20] impregnated carbon fibers with $Fe(NO_3)_3$ followed by precipitation, and loaded gold using $Au(en)_2Cl_3$ precursor. The Au/FeO_x/C exhibited some activity in CO oxidation but quickly deactivated [20]. Rønning and coworkers [21,22] modified carbon nanofibers by TiO_2 nanoparticles and loaded gold by two methods. The deposition–precipitation method led to large gold particles (>50 nm), whereas the colloidal dispersion led to smaller gold particles (6 nm). The Au/TiO_2/C synthesized via dispersion of gold colloids showed activity in the water–gas shift reaction, but no data on CO oxidation were reported [22].

To design surface-modified carbon-based gold catalysts, it is essential to properly introduce the modifier so as to avoid the mechanical segregation of the modifier and carbon and achieve the catalytic synergistic effect of gold and the modifier. Recently, there has been great interest in the electroless deposition of MnO_x on carbon electrodes achieved by immersing carbon in an aqueous $KMnO_4$ or $NaMnO_4$ [23–29]. This practice results in the conformal coating of MnO_x on carbon with the sacrificial oxidation of carbon surface ($4KMnO_4 + 3C + 2H_2O \rightarrow 4MnO_2 + 3CO_2 + 4KOH$) [29]. The objective of these studies is to develop high-performance MnO_x/C capacitors as energy-storage devices; however, to the best of our knowledge, these novel materials have not yet been used for preparing supported gold catalysts. Herein we report the preparation of gold particles on MnO_x/C, along with the characterization, activity, and stability of Au/MnO_x/C in CO oxidation. The promotional effect of MnO_x is established.

* Corresponding author. Fax: +1 865 576 5235.
E-mail address: dais@ornl.gov (S. Dai).

0021-9517/$ – see front matter Published by Elsevier Inc.
doi:10.1016/j.jcat.2007.08.013

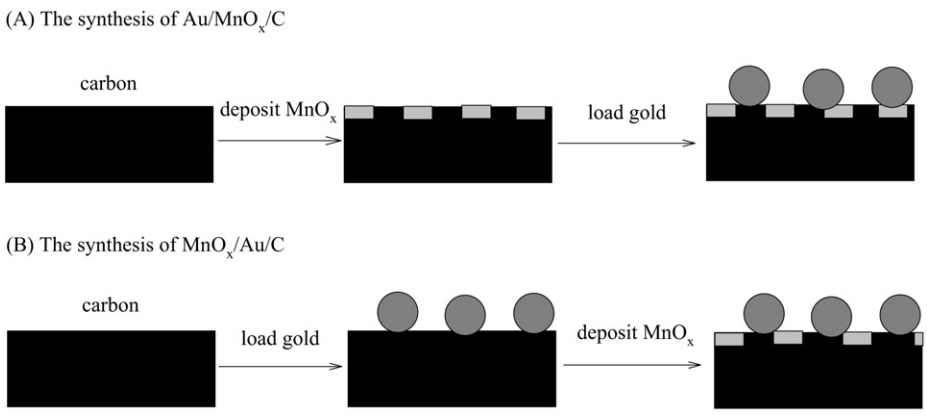

Fig. 1. Simplified schemes for the preparation of Au/MnO_x/C (route A) and MnO_x/Au/C (route B) involving the reaction between $KMnO_4$ and carbon ($4KMnO_4 + 3C + 2H_2O \rightarrow 4MnO_2 + 3CO_2 + 4KOH$).

2. Experimental

To prepare MnO_x/C, 2 g of carbon (C1: carbopack, Supelco Inc.; C2: carbon black powder, VXC-72R, Carbot; C3: activated charcoal; C4: Nuchar, RGC 40) was dispersed in 90 mL of deionized water under magnetic stirring, and 10 mL of 0.5 M $KMnO_4$ poured into the beaker. The magnetic stirring was continued for 1 h unless otherwise indicated. The suspension was centrifuged, washed thoroughly with water, and dried at 85 °C overnight. For comparison, MnO_x was prepared by calcining $Mn(NO_3)_2{\cdot}xH_2O$ at 500 °C for 3 h, and MnO_x/TiO_2 was prepared by impregnating TiO_2 (Degussa P25) with $Mn(NO_3)_2$, with an intended loading of 0.1 g MnO_x per g of TiO_2, followed by drying and calcination.

To load gold, 0.3 g of $HAuCl_4{\cdot}3H_2O$ was dissolved into 50 mL of water. The pH value was adjusted to 10.0 using 1.0 M KOH, and the solution was heated to 80 °C, followed by the addition of 1.0 g of support. The mixture was stirred for 2 h, after which the precipitates were separated by centrifugation and washed four times with water. The product was dried at 40 °C to obtain the as-synthesized catalyst (Fig. 1, route A). For comparison, MnO_x/Au/C-1 was prepared by treating 0.5 g of Au/C-1 with an aqueous $KMnO_4$ (22.5 mL of water + 2.5 mL of 0.5 M $KMnO_4$) for 1 h, followed by washing and then drying at 85 °C overnight (Fig. 1, route B).

CO oxidation was tested in a plug-flow microreactor (Altamira AMI 200). Unless otherwise indicated, 50 mg of catalyst was loaded into a U-shaped quartz tube (4 mm i.d.) and pretreated in flowing 5% O_2 (balance He) at 200 or 500 °C for 2.5 h. After the catalyst was cooled, the gas stream was switched to 1% CO (balanced air, flow rate of 37 cm^3/min), and the reaction temperature was ramped using a furnace or by immersing the U-shaped tube in ice water or acetone-liquid nitrogen. The product was analyzed using a gas chromatograph with a thermal conductivity detector, and CO conversion was calculated as $X_{CO} = [CO_2]_{out}/([CO]_{out} + [CO_2]_{out})$.

XRD data were collected on a Siemens D5005 diffractometer with CuK_α radiation. The average gold particle sizes were estimated by applying the Debye–Scherrer equation on the Au(111) diffraction ($2\theta = 38°$). BET surface areas were measured by N_2 adsorption–desorption using a Micromeritics Gemini instrument. The Au and Mn content was measured by ICP-OES on a Thermo IRIS Intrepid II spectrometer. SEM, TEM, and EDX experiments were conducted on a Hitachi HD-2000 STEM instrument operated at 200 kV.

3. Results

Fig. 2A shows CO conversions on samples pretreated at 200 °C. Au/C-1 was inactive, but Au/MnO_x/C-1 was active, achieving almost complete conversion at 100 °C. The CO conversion on Au/MnO_x/C-1 is not due to the artifact caused by the combustion of carbon, because the catalyst was pretreated in O_2–He before reaction testing, and the reaction temperature was lower than the pretreatment temperature. In addition, the experiment was rechecked by passing air through the pretreated Au/MnO_x/C-1 at the reaction temperature; no CO_2 formation was detected. The specific rates of Au/C-1 and Au/MnO_x/C-1 at 80 °C were calculated as 0.03 and 0.17 mol/(g_{Au} h), respectively. In one control experiment, MnO_x/C-1 was found to be inactive below 120 °C (Fig. 2A). In another control experiment, MnO_x/Au/C-1 prepared by soaking Au/C-1 in a $KMnO_4$ solution showed lower conversion than that of Au/MnO_x/C-1 but still higher than that of Au/C-1 (Fig. 2A). Therefore, preparation sequence (Au/MnO_x/C-1 vs MnO_x/Au/C-1) matters, and the Au–MnO_x interface in Au/MnO_x/C-1 and MnO_x/Au/C-1 is important, whereas both the MnO_x–C and Au–C combinations are much less active.

Fig. 2B shows XRD data for the supports and as-synthesized catalysts. C-1 showed graphite peaks. After loading gold on C-1, sharp gold peaks appeared at $2\theta = 38, 44, 65, 78$, and 82°, and the average gold particle size was estimated as 22 nm by XRD. For MnO_x/C-1, no crystalline MnO_x was detected, indicating the dispersion of MnO_x [27]. In an earlier study [27], XPS data demonstrated that the oxidation state of Mn is +4. Once gold was loaded onto MnO_x/C-1, the gold peaks were sharp, and the estimated average gold particle size was 22 nm. The accuracy of this estimate was checked by TEM, as shown in Fig. 3.

To explore whether these trends are general, we tried different carbons. As shown in Figs. S1–S3 and Table S1, in supporting information, the modification of carbons by MnO_x always

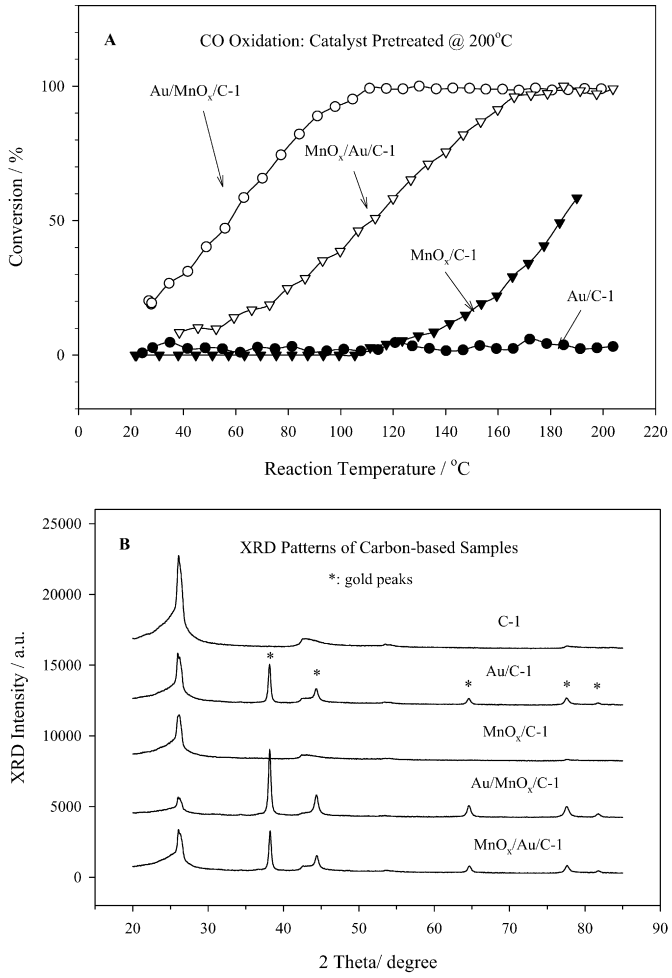

Fig. 2. Panel A: CO conversion curves of 200 °C-pretreated Au/C-1, Au/MnO_x/C-1, MnO_x/C-1, and MnO_x/Au/C-1. Panel B: XRD patterns of as-obtained C-1 and as-synthesized Au/C-1, Au/MnO_x/C-1, MnO_x/C-1, and MnO_x/Au/C-1.

promoted CO oxidation but did not significantly decrease the average gold particle size, as revealed by XRD. We also treated C-1 by $KMnO_4$ for longer durations (3–24 h), and found that CO conversion was slightly increased and the gold peaks were still sharp (Fig. S4 and Table S2, in supporting information). There could be carbon sites uncovered by MnO_x, leading to the reaction between Au^{3+} and the reductive carbon to form a proportion of large gold particles [30] that had biased the XRD results.

Representative dark-field TEM images of samples collected after the pretreatment at 200 °C and reaction testing are shown in Fig. 3. For Au/C-1, there were large gold particles (on the order of 20–100 nm) on carbon, along with numerous 2–4 nm gold clusters (bright dots) (Figs. 3B and S5). We selected an area with bright dots but without large gold particles and performed an EDX scan, which revealed carbon and gold with no other heavy elements (data not shown). In contrast, we found no similar bright dots on neat C-1 support (Fig. 3A). Therefore, the TEM data show that the XRD data (Fig. 2B) of Au/C-1 were biased by a small proportion of large gold particles.

For Au/MnO_x/C-1, SEM showed similar morphology for Au/MnO_x/C-1 and MnO_x-free C-1, and no MnO_x agglomerates (data not shown). Dark-field TEM images showed the dominance of 4–10 nm gold nanoparticles, together with a small proportion of larger (20–100 nm) gold particles (Figs. 3C and S6, and other images not shown). Therefore, the gold particle sizes estimated by XRD (Tables S1 and S2) were biased by large gold particles [31]. We selected a gold particle for EDX analysis and found gold, manganese, and carbon (Fig. 4). We also selected another area without gold particles and found manganese and carbon, but no gold (Fig. 4). These findings indicate that MnO_x is dispersed on the carbon surface, and the presence of Au–MnO_x interfaces is important for achieving high activity.

For MnO_x/Au/C-1, TEM data indicated large gold particles (on the order of 20–100 nm) without observable gold clusters (Fig. 3D and other images not shown). This finding stands in contrast to the presence of numerous gold nanoclusters on Au/C-1 (Fig. 3B) and the dominance of gold nanoparticles (4–10 nm) on Au/MnO_x/C-1 (Fig. 3C). Therefore, the synthesis sequence (MnO_x/Au/C-1 vs Au/MnO_x/C-1) affects gold distribution. For Au/MnO_x/C-1, gold was loaded onto presynthesized MnO_x/C-1 without interference from the chemical reaction between $KMnO_4$ and carbon (Fig. 1, route A); however, for MnO_x/Au/C-1, Au/C-1 was soaked in an aqueous $KMnO_4$ (Fig. 1, route B). The corrosion reaction may loosen the attachment between gold clusters and the carbon support, causing the leaching of small gold clusters. Because large gold particles (e.g., 20–100 nm) in Au/C-1 occupied patches of carbon sites, they were left behind. This finding is supported by the TEM data (compare Fig. 3B and 3D) and also by the elemental analysis results, which showed a lower gold content for MnO_x/Au/C-1 (1.0 wt%) than for Au/C-1 (2.0 wt%).

To put the present work in its proper context, we compared Au/MnO_x/C-1 with Au/MnO_x [32–36] and Au/MnO_x/TiO_2 [37]. As identified by XRD (Fig. S7), the MnO_x formed by decomposing $Mn(NO_3)_2$ was Mn_3O_4 [38]. MnO_x/TiO_2 exhibited anatase and rutile phases but no crystalline MnO_x, implying that the MnO_x was highly dispersed [37]. In contrast to Au/C-1 and Au/MnO_x/C-1 (Fig. 2B), as-synthesized Au/MnO_x and Au/MnO_x/TiO_2 exhibited virtually no gold peaks, implying the dispersion of small gold species.

As shown in Fig. 5, the activity of Au/MnO_x/C-1 was lower than that of Au/MnO_x and Au/MnO_x/TiO_2 and was decreased after pretreating Au/MnO_x/C-1 at 500 °C. At such high pretreatment temperature in O_2–He, a portion of the carbon material was combusted, as revealed by visual inspection of the catalyst bed after pretreatment. In contrast, the carbon material in Au/C-1 was not combusted at 500 °C. The MnO_x coating may catalyze the oxidation of carbon at elevated pretreatment temperatures [27]. For reference, the catalytic activities of 1 wt% Au/TiO_2 and 0.8 wt% Au/Al_2O_3 obtained from AuTEK also are reported in Fig. 5.

The TEM images of Au/MnO_x and Au/MnO_x/TiO_2 were recorded. Au/MnO_x contained numerous distributed 3–10 nm gold nanoparticles with virtually no larger gold particles (Fig. 3E). For Au/MnO_x/TiO_2, the gold particle sizes were nor-

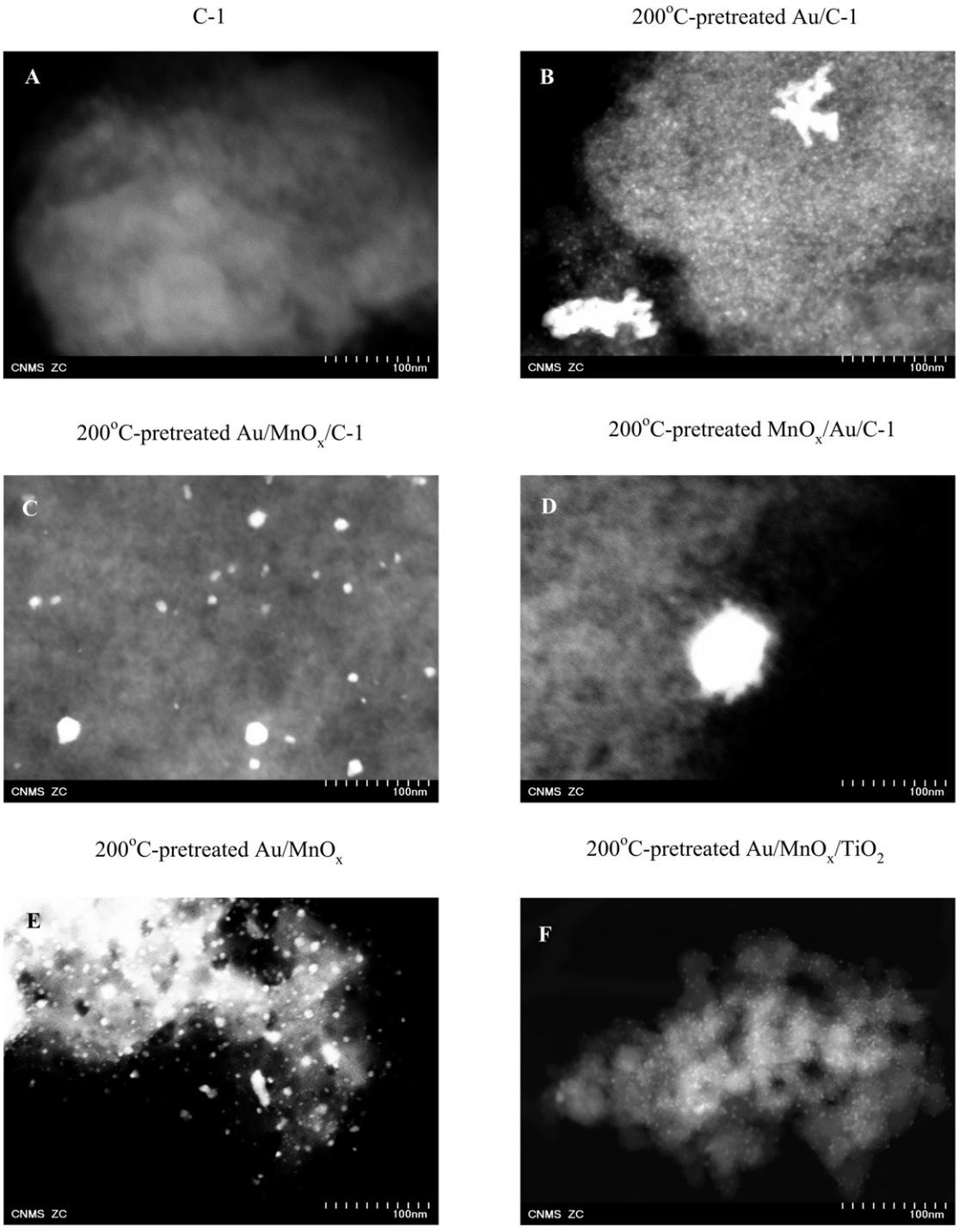

Fig. 3. Z-contrast TEM images of C-1 and 200 °C-pretreated Au/C-1, $Au/MnO_x/C$-1, $MnO_x/Au/C$-1, Au/MnO_x, and $Au/MnO_x/TiO_2$ collected after CO reaction.

mally in the range of 2–4 nm (Figs. 4F and S7), consistent with its high activity in CO oxidation.

The temporal stability of the $Au/MnO_x/C$-1, Au/MnO_x, and $Au/MnO_x/TiO_2$ pretreated at 200 °C is compared in Fig. 6. To properly test the stability, we adjusted the mass of catalyst ($Au/MnO_x/TiO_2$) to ensure that conversion was <100%, because observing 100% conversion all of the time does not mean that the catalyst is stable [5]. On the other hand, because three catalysts exhibited completely different activity (Fig. 5A), each of these catalysts' stability was tested at different temperatures (80, 55, and 23 °C, respectively), to avoid the scenario in which at the same temperature, the conversion on one catalyst is always 100% and that on another is always close to zero. To test the stability of different catalysts at different temperatures according to the activity is a common practice adopted by others [39–41] and us [42,43].

As shown in Fig. 6, the activity of $Au/MnO_x/C$-1 at 80 °C was fairly stable on stream, consistent with the good tempo-

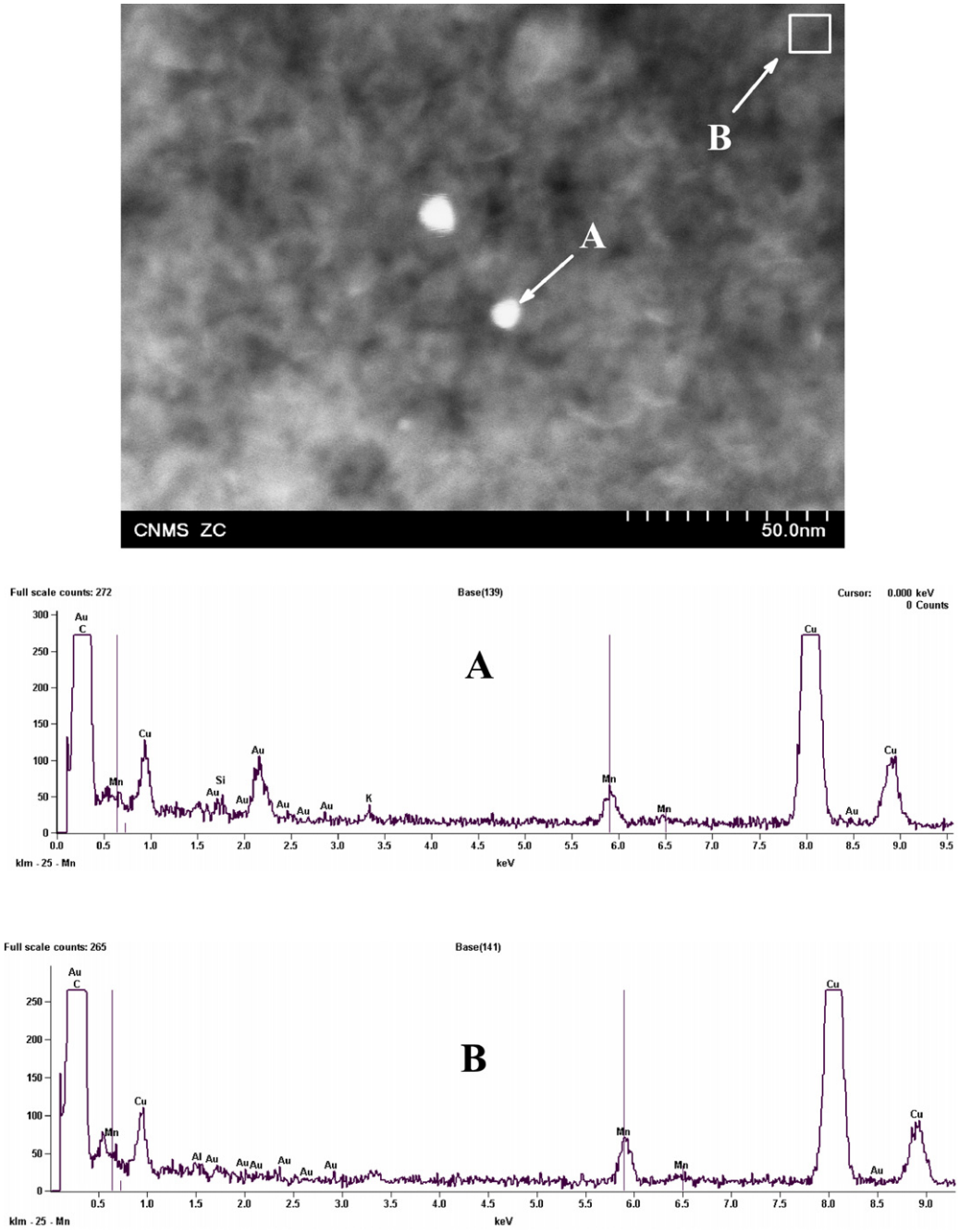

Fig. 4. EDX results of selected areas of 200 °C-pretreated Au/MnO_x/C-1.

ral stability of Au/MnO_x reported in the literature [32–36]. The stability of Au/MnO_x at 55 °C and Au/MnO_x/TiO_2 at 23 °C was still acceptable. No comment was given concerning whether the stability of Au/MnO_x/C-1 was better than that of Au/MnO_x or Au/MnO_x/TiO_2 because the former was prepared using $KMnO_4$ precursor whereas the latter were prepared by decomposing $Mn(NO_3)_2$. We previously showed that Au/ZnO/TiO_2 and Au/La_2O_3/TiO_2 prepared using metal nitrates as the precursor deactivated quickly on stream, probably due to the accumulation of carbonate species [42]. The premise that the stability of Au/MnO_x/C-1 at 80 °C (Fig. 6) is not due to the relatively high reaction temperature can be questioned, so we repeated the experiment at 21 and 50 °C, respectively (bottom two traces in Fig. 6); the activity of Au/MnO_x/C-1 was good.

4. Discussion

Although Au/C may show some activity in CO oxidation (Figs. S1 and S3) [17], the activity is much lower than that of Au/TiO_2, which shows complete CO conversion below room temperature [44]. One reason for this may be that gold particles on carbon are large due to the reaction between Au^{3+} and reductive carbon surfaces during preparation [7,30]. If this were

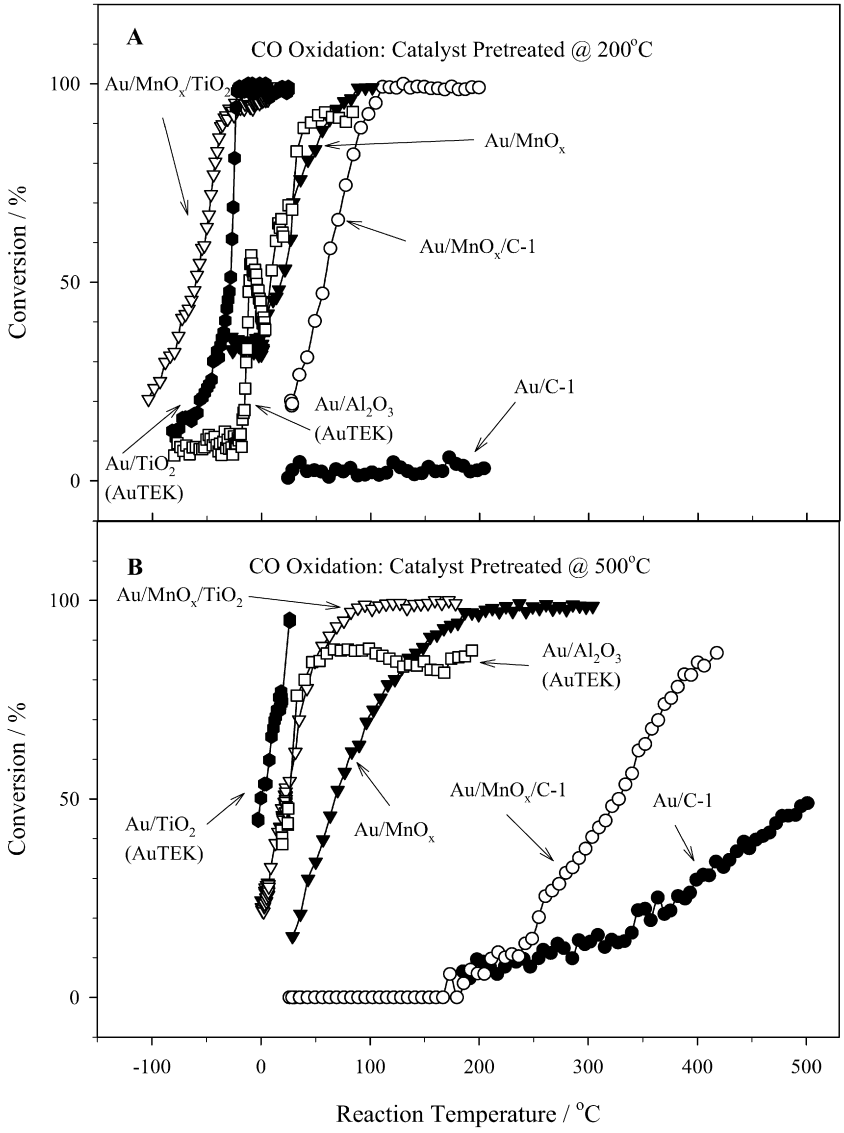

Fig. 5. CO conversion curves of Au/C-1, Au/MnO_x/C-1, Au/MnO_x, Au/MnO_x/TiO_2, 1 wt% Au/TiO_2 (AuTEK), and 0.8 wt% Au/Al_2O_3 (AuTEK). The catalysts were pretreated at 200 (A) or 500 °C (B) before the reaction testing.

the only reason, then one should be able to make Au/C very active by assembling small gold particles on carbon; however, we have shown that in addition to large gold particles that biased the XRD peaks, there were numerous gold nanoclusters on Au/C-1 (Figs. 2B and 3B) [31], but still Au/C-1 was not active for CO oxidation. Davis and coworkers [14,15] deposited gold nanoparticles on carbon via colloidal dispersion and found that these Au/C samples were not active for gas-phase CO oxidation. Interestingly, Veith et al. [12] deposited gold nanoclusters on carbon via physical vapor deposition, but our group tested the Au/C catalyst furnished by this group and found that it was not active for CO oxidation. Therefore, large gold chunks are supposed to be inactive for CO oxidation, but the presence of small gold clusters or nanoparticles on carbon is not a sufficient condition for achieving high activity in low-temperature gas-phase CO oxidation.

Another reason for the low activity of Au/C compared with Au/TiO_2 in CO oxidation could be that carbon is an "inert" support [14–19], whereas TiO_2 is an "active" support thought to activate and store oxygen [45]. Although the mechanisms of CO oxidation are not completely understood, a viable mechanism is that gold nanoparticles activate CO, the support activates oxygen, and the reaction occurs at the gold–support interface [5]. Recently, Davis and coworkers [14,15] found that Au/C samples were not active for gas-phase CO oxidation, but were active for liquid-phase CO oxidation in the presence of an aqueous base to activate oxygen. Lu et al. [19] observed enhanced activity in selective CO oxidation in H_2-rich stream by impregnating Au/C with KNO_3 and proposed that one role of K is to keep the gold nanoparticles small and the other role is to provide an "oxygen attractor." According to this reasoning, suitable reaction media [14,15] or specific promoters [19] are needed to activate oxygen so as to make the inactive Au/C catalysts active for CO oxidation.

In the present work, we used MnO_x to modify Au/C catalysts. The role of MnO_x is believed to provide an Au–MnO_x

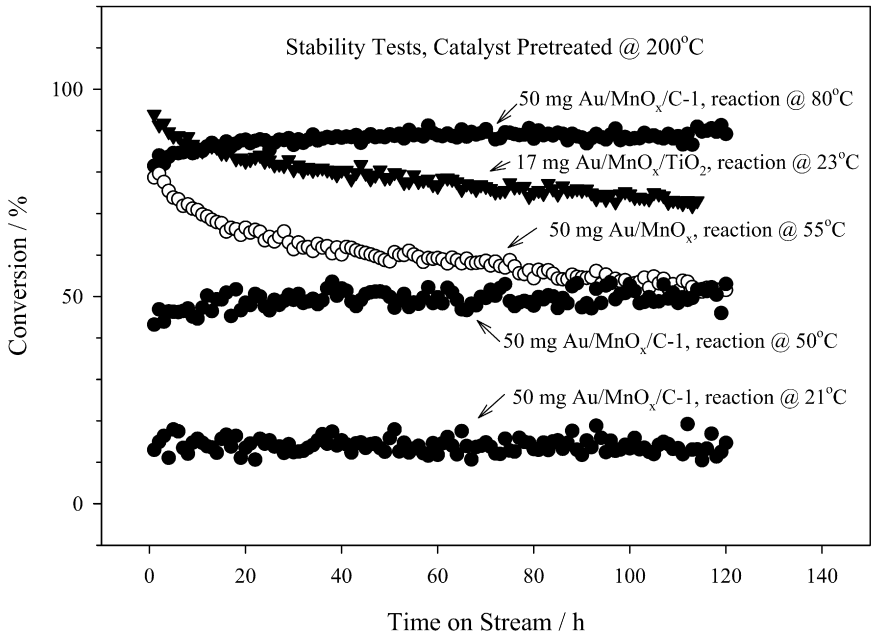

Fig. 6. Stability of $Au/MnO_x/C$-1, Au/MnO_x, and $Au/MnO_x/TiO_2$ as a function of time on stream.

interface active for the oxygen interaction sites necessary for CO oxidation. It has been reported that Au/MnO_x catalysts are active for CO oxidation [32–36] and VOC combustion [46], and that the role of MnO_x in $Au/MnO_x/Al_2O_3$ [47] and $Au/MnO_x/TiO_2$ [37] is to supply reaction oxygen. In the present work, the beneficial effect of the Au–MnO_x interface is supported not only by control experiments on the catalytic activity of Au/C, MnO_x/Au/C, MnO_x/C (Fig. 2A), and Au/MnO_x (Fig. 5), but also by TEM and EDX data (Fig. 4). In general terms, the interfaces between gold and active metal oxides are important for CO oxidation. For example, Bollinger and Vannice [48] deposited TiO_x onto an inactive gold powder and reported high activity in CO oxidation, and Horváth et al. [49] modified inactive Au/SiO_2 with active TiO_2 patches to create new Au–TiO_2 interfaces active for CO oxidation. Therefore, the new $Au/MnO_x/C$ catalysts benefit from the high activity of the Au–MnO_x interface [32–37,46,47].

To the best of our knowledge, this is the first report on the synthesis, characterization, and catalytic CO oxidation of $Au/MnO_x/C$ synthesized by electroless deposition. El-Deab and Ohsaka recently used electrochemical methods to deposit gold particles (on the order of 100 nm) and MnO_x nanoparticles onto carbon electrodes for electrochemical reduction of oxygen [50,51]. The deposition method, the sizes of the gold and MnO_x, and the morphology of the catalysts differ from those in our $Au/MnO_x/C$ system. Our work provides a way in which carbon materials can be used for preparing active gold catalysts through proper surface functionalization by an "active" metal oxide promoter, which is evasive in the literature [5]. In view of the electrical conductivity of MnO_x/C [23–29] and the redox properties of MnO_x [38], further electrocatalytic work can be conducted and the applications of $Au/MnO_x/C$ in other reactions can be surveyed.

5. Conclusion

In this work, $Au/MnO_x/C$ catalysts were prepared by modifying carbons by MnO_x via an electroless deposition approach, followed by loading gold via a deposition–precipitation method. The $Au/MnO_x/C$ catalysts exhibited enhanced activity in CO oxidation compared with the corresponding Au/C samples. The presence of the Au–MnO_x interface is important for CO oxidation, and the unique electroless deposition method provides a good means for the conformal coating of MnO_x on carbon substrates. The $Au/MnO_x/C$ catalyst system combines the high activity and temporal stability of the Au–MnO_x interface.

Acknowledgments

This work was supported by the U.S. Department of Energy's BES Program (DE-AC05-00OR22725). Z.M. thanks the ORNL-ORAU Research Associates Program. The 1 wt% Au/TiO_2 and 0.8 wt% Au/Al_2O_3 were donated by Dr. Jason MacPherson of AuTEK. The helpful suggestions of anonymous reviewers are greatly appreciated.

Supporting information

The online version of this article contains additional supporting information.

Please visit doi: 10.1016/j.jcat.2007.08.013.

References

[1] D.T. Thompson (Ed.), Special Issue—Gold Catalysis, Catal. Today 72 (1–2) (2002) 1–169.

[2] G.J. Hutchings, M. Haruta (Eds.), Special Issue: Catalysis by Gold, Appl. Catal. A Gen. 291 (1–2) (2005) 1–262.

[3] B. Nieuwenhuys, J. Ross (Eds.), Gold 2006: New industrial applications for gold-selected papers on catalysis from the 4th International Conference on Gold Science, Technology and Its Applications, University of Limerick, Ireland, September 3–6, 2006, Catal. Today, vol. 122, 2007, pp. 195–412.
[4] G.J. Hutchings, W. Goodman (Eds.), Catalysis by Gold, Top. Catal. 44 (3–4) (2007) 1–343.
[5] G.C. Bond, C. Louis, D.T. Thompson, Catalysis by Gold, Imperial College Press, London, 2006.
[6] L.R. Radovic, F. Rodriguez-Reinoso, Chem. Phys. Carbon 25 (1997) 243.
[7] L. Prati, G. Martra, Gold Bull. 32 (1999) 96.
[8] C.L. Bianchi, S. Biella, A. Gervasini, L. Prati, M. Rossi, Catal. Lett. 85 (2003) 91.
[9] S. Demirel-Gülen, M. Lucas, P. Claus, Catal. Today 102 (2005) 166.
[10] M.D. Hughes, Y.-J. Xu, P. Jenkins, P. McMorn, P. Landon, D.I. Enache, A.F. Carley, G.A. Attard, G.J. Hutchings, F. King, E.H. Stitt, P. Johnston, K. Griffin, C.J. Kiely, Nature 437 (2005) 1132.
[11] G.J. Hutchings, S. Carrettin, P. Landon, J.K. Edwards, D. Enache, D.W. Knight, Y.J. Xu, A.F. Carley, Top. Catal. 38 (2006) 223.
[12] G.M. Veith, A.R. Lupini, S.J. Pennycook, A. Villa, L. Prati, N.J. Dudney, Catal. Today 122 (2007) 248.
[13] C. Baatz, N. Thielecke, U. Prüße, Appl. Catal. B 70 (2007) 653.
[14] W.C. Ketchie, M. Murayama, R.J. Davis, Top. Catal. 44 (2007) 307.
[15] W.C. Ketchie, Y.-L. Fang, M.S. Wong, M. Murayama, R.J. Davis, J. Catal. 250 (2007) 95.
[16] M. Okumura, S. Tsubota, M. Haruta, J. Mol. Catal. A 199 (2003) 73.
[17] D.A. Bulushev, I. Yuranov, E.I. Suvorova, P.A. Buffat, L. Kiwi-Minsker, J. Catal. 224 (2004) 8.
[18] L.A. Brey, T.E. Wood, G.M. Buccellato, M.E. Jones, C.S. Chamberlain, A.R. Siedle, Catalysts, activating agents, support media, and related methodologies useful for making catalyst systems especially when the catalyst is deposited onto the support media using physical vapor deposition, WO 2005/030382, 2005.
[19] F. Wang, G.X. Lu, Catal. Lett. 115 (2007) 46.
[20] D.A. Bulushev, L. Kiwi-Minsker, I. Yuranov, E.I. Suvorova, P.A. Buffat, A. Renken, J. Catal. 210 (2002) 149.
[21] N. Hammer, I. Kvande, D. Chen, M. Rønning, Catal. Today 122 (2007) 365.
[22] N. Hammer, I. Kvande, X. Xu, V. Gunnarsson, B. Totdal, D. Chen, M. Rønning, Catal. Today 123 (2007) 245.
[23] H.Y. Lee, S.W. Kim, H.Y. Lee, Electrochem. Solid State Lett. 4 (2001) A19.
[24] M.Q. Wu, G.A. Snook, G.Z. Chen, D.J. Fray, Electrochem. Commun. 6 (2004) 499.
[25] H. Kawaoka, M. Hibino, H. Zhou, I. Honma, Solid State Ionics 176 (2005) 621.
[26] S.B. Ma, Y.H. Lee, K.Y. Ahn, C.M. Kim, K.H. Oh, K.B. Kim, J. Electrochem. Soc. 153 (2006) C27.
[27] X.P. Dong, W.H. Shen, J.L. Gu, L.M. Xiong, Y.F. Zhu, H. Li, J.L. Shi, Microporous Mesoporous Mater. 91 (2006) 120.
[28] A.E. Fischer, K.A. Pettigrew, D.R. Rolison, R.M. Stroud, J.W. Long, Nano Lett. 7 (2007) 281.
[29] X.K. Huang, H.J. Yue, A. Attia, Y. Yang, J. Electrochem. Soc. 154 (2007) A26.
[30] P.A. Simonov, V.A. Likholobov, in: A. Wieckowski, E.R. Savinova, C.G. Vayenas (Eds.), Catalysis and Electrocatalysis at Nanoparticle Surfaces, Marcel Dekker, New York, 2003, p. 409.
[31] P. Riello, P. Canton, A. Benedetti, Langmuir 14 (1998) 6617.
[32] S.D. Gardner, G.B. Hoflund, B.T. Upchurch, D.R. Schryer, E.J. Kielin, J. Schryer, J. Catal. 129 (1991) 114.
[33] G.B. Hoflund, S.D. Gardner, D.R. Schryer, B.T. Upchurch, E.J. Kielin, Appl. Catal. B 6 (1995) 117.
[34] R.M.T. Sanchez, A. Ueda, K. Tanaka, M. Haruta, J. Catal. 168 (1997) 125.
[35] S.-J. Lee, A. Gavriilidis, Q.A. Pankhurst, A. Kyek, F.E. Wagner, P.C.L. Wong, K.L. Yeung, J. Catal. 200 (2001) 298.
[36] A. Luengnaruemitchai, D.T.K. Thoa, S. Osuwan, E. Gulari, Int. J. Hydrogen Energ. 30 (2005) 981.
[37] L.-H. Chang, N. Sasirekha, Y.-W. Chen, Catal. Commun. 8 (2007) 1702.
[38] A. Chen, H. Xu, Y. Yue, W. Hua, W. Shen, Z. Gao, J. Mol. Catal. A 203 (2003) 299.
[39] E.D. Park, J.S. Lee, J. Catal. 186 (1999) 1.
[40] T.V. Choudhary, C. Sivadinarayana, C.C. Chusuei, A.K. Datye, J.P. Fackler, D.W. Goodman, J. Catal. 207 (2002) 247.
[41] S.-H. Wu, X.-C. Zheng, S.-R. Wang, D.-Z. Han, W.-P. Huang, S.-M. Zhang, Catal. Lett. 96 (2004) 49.
[42] Z. Ma, S.H. Overbury, S. Dai, J. Mol. Catal. A 273 (2007) 186.
[43] Z. Ma, S. Brown, S.H. Overbury, S. Dai, Appl. Catal. A 327 (2007) 226.
[44] H.G. Zhu, Z. Ma, S.H. Overbury, S. Dai, Catal. Lett. 116 (2007) 128.
[45] M.M. Schubert, S. Hackenberg, A.C. van Veen, M. Muhler, V. Plzak, R.J. Behm, J. Catal. 197 (2001) 113.
[46] A.K. Sinha, K. Suzuki, M. Takahara, H. Azuma, T. Nonaka, K. Fukumoto, Angew. Chem. Int. Ed. 46 (2007) 2891.
[47] R.J.H. Grisel, B.E. Nieuwenhuys, J. Catal. 199 (2001) 48.
[48] M.A. Bollinger, M.A. Vannice, Appl. Catal. B 8 (1996) 417.
[49] A. Horváth, A. Beck, A. Sárkány, G. Stefler, Z. Varga, O. Geszti, L. Tóth, L. Guczi, J. Phys. Chem. B 110 (2006) 15417.
[50] M.S. El-Deab, T. Ohsaka, J. Electrochem. Soc. 153 (2006) A1365.
[51] M.S. El-Deab, T. Ohsaka, Electrochim. Acta 52 (2007) 2166.